

## Article

# Lithium Extraction from Lithium-Bearing Clay Minerals by Calcination-Leaching Method

Jie Liu <sup>1,2</sup>, Rui Xu <sup>1,2</sup>, Wei Sun <sup>1,2,\*</sup>  and Ye Zhang <sup>3,\*</sup>

<sup>1</sup> School of Minerals Processing and Bioengineering, Central South University, Changsha 410083, China; 215611056@csu.edu.cn (J.L.); rxrui@csu.edu.cn (R.X.); sunmenghu@csu.edu.cn (W.S.)

<sup>2</sup> Key Laboratory of Hunan Province for Clean and Efficient Utilization of Strategic Calcium-Containing Mineral Resources, Central South University, Changsha 410083, China

<sup>3</sup> National Engineering Research Center for Comprehensive Utilization of Salt Lake Resources, School of Chemical Engineering, East China University of Science and Technology, Shanghai 200237, China

\* Correspondence: li\_wang@csu.edu.cn (L.W.); zhangye@ecust.edu.cn (Y.Z.)

**Abstract:** Lithium is a significant energy metal. This study focuses on the extraction of lithium from lithium-bearing clay minerals utilizing calcination combined with oxalic acid leaching. The relevant important parameters, leaching kinetics analysis, and the lithium extraction mechanism were deeply investigated. The results demonstrate that a high lithium recovery of 91.35% could be achieved under the optimal conditions of calcination temperature of 600 °C, calcination time of 60 min, leaching temperature of 80 °C, leaching time of 180 min, oxalic acid concentration of 1.2 M, and liquid-to-solid ratio of 8:1. According to the shrinkage core model, the leaching kinetics of lithium using oxalic acid followed a chemical reaction-controlled process. XRD, TG, and SEM analysis showed that the kaolinite, boehmite, and diaspore phases in raw ore transformed into corundum, quartz, and muscovite phase in calcination products when the calcination temperature was higher than 600 °C. Moreover, the expansion of the interlayer spacing of minerals during the calcination process could promote the lithium release. During the leaching process, lithium present in the layered silicates was efficiently recovered through ion exchange with the dissociated H<sup>+</sup> from oxalic acid. This study could provide a promising guide for lithium extraction from lithium-bearing clay minerals.

**Keywords:** lithium extraction; clay minerals; calcination; oxalic acid leaching



**Citation:** Liu, J.; Xu, R.; Sun, W.; Wang, L.; Zhang, Y. Lithium Extraction from Lithium-Bearing Clay Minerals by Calcination-Leaching Method. *Minerals* **2024**, *14*, 248. <https://doi.org/10.3390/min14030248>

Academic Editors: Bogale Tadesse, Jonas Addai-Mensah, Girma Woldehinsae and Lisha Dong

Received: 24 January 2024  
Revised: 20 February 2024  
Accepted: 26 February 2024  
Published: 28 February 2024



**Copyright:** © 2024 by the authors. Licensee MDPI, Basel, Switzerland. This article is an open access article distributed under the terms and conditions of the Creative Commons Attribution (CC BY) license (<https://creativecommons.org/licenses/by/4.0/>).

## 1. Introduction

Lithium holds vital significance as an indispensable constituent within rechargeable batteries, fuel cells, and electronic devices [1]. The escalating production of electric vehicles poses a potential increase in demand for lithium resources in the forthcoming decades [2]. Lithium was traditionally recovered from brine, pegmatite lithium mines, and sedimentary lithium mines [3]. As a potential lithium resource, lithium-bearing clay minerals have recently attracted great attention and could be used to provide a promising strategy to meet the lithium demand [4].

Currently, lithium extraction methods from lithium-bearing clay minerals include direct leaching, chlorination-sulphuration, and assisted roasting leaching [5]. It has been shown that direct water leaching yields a low lithium extraction rate of less than 1%, while direct sulfuric acid leaching could achieve an 89% of lithium extraction rate with the consumption of 0.56 kg of sulfuric acid per kilogram of lithium-bearing clay minerals, leading to issues of equipment corrosion and high cost [6]. The chlorination-sulphuration method involves the use of significant amounts of harmful gases and can extract 85.8% of lithium when consuming 0.45 kg of SO<sub>2</sub> per kilogram of lithium-bearing clay minerals. However, this method suffers from poor operability and safety issues [7]. In contrast, the assisted roasting leaching method has gained widespread application in lithium extraction from clay minerals owing to its simplicity and high extraction rate. For example, by using 50 g

of calcium sulfate as an assisting agent, a high lithium extraction rate of 72% could be yield under the conditions of 100 g of lithium-bearing clay minerals, 1000 °C of temperature, and 4 h of time [5]. However, the addition of assisting agents increases the amount of residue remaining after leaching, making waste residue disposal more challenging. To address this issue, Hannian Gu et al. [8] studied lithium extraction from lithium-rich aluminum clay ores and directly calcined the raw ores without adding assisting agents at 500 °C and 600 °C, followed by leaching with sulfuric acid. The resulting lithium extraction rates were 72.34% and 73.61%, respectively. Wencai Zhang et al. [9] conducted a leaching experiment using 1.2 M hydrochloric acid at a reaction temperature of 75 °C. The lithium recovery from clay minerals was less than 10%. However, after combination of calcination at 600 °C, the lithium recovery significantly increased to 70%–80%. Evidently, calcination treatment can effectively activate lithium-bearing clay minerals, making lithium exchangeable. Moreover, compared to assisted roasting, calcination is generally conducted at lower temperatures without additional assisting agents, which is beneficial for green production.

This research focuses on lithium extraction from lithium-bearing clay minerals utilizing the calcination-leaching method. Conventional inorganic acids, such as sulfuric acid and hydrochloric acid, are known for their high corrosiveness and the potential release of harmful gases, such as  $\text{Cl}_2$ ,  $\text{SO}_3$ , and  $\text{NO}_x$ , during the leaching process [10]. Therefore, this study employed oxalic acid, an organic acid, as the leaching agent. Furthermore, the produced lithium oxalate is one of the raw materials that can be used in the preparation of the high-performance lithium battery electrolyte, lithium difluoro(oxalato)borate (LiODFB) [11]. At the same time, lithium oxalate itself can also be utilized as a cathode material for lithium storage batteries. The influence factors, kinetics, and the mechanisms involved in the calcination and leaching processes are thoroughly investigated.

## 2. Materials and Methods

### 2.1. Materials

The lithium-bearing clay minerals were taken from Yunnan Province, China. As shown in Figure 1, this mineral primarily comprised chlorite, kaolinite, diaspore, muscovite, and boehmite, with a minor proportion of anatase. The predominant chemical composition comprised 0.75% of  $\text{Li}_2\text{O}$ , 48.36% of  $\text{Al}_2\text{O}_3$ , 28.53% of  $\text{SiO}_2$ , 2.53% of  $\text{Fe}_2\text{O}_3$ , and 10.11% of  $\text{K}_2\text{O}$ .

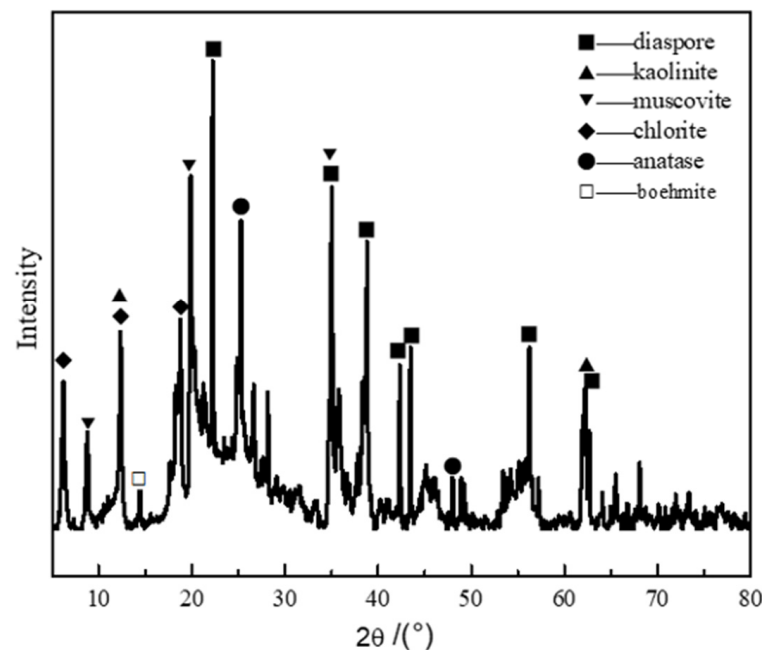


Figure 1. XRD result of the lithium-bearing clay minerals.

## 2.2. Experiments

During the calcination-leaching experiments, 150 g of mineral samples ground with a cone ball mill (XMQ-240\*90, Jiangxi WKD, Ganzhou, China) were placed in a muffle furnace (KSL-1200X, Shanghai Yiheng, Shanghai, China) and calcinated for a certain time at various temperatures. Then, the calcinated samples were put into the oxalic acid solution for leaching at a certain condition. After leaching and filtration, the residue and filtrate could be obtained. The lithium concentration in filtrate was measured using an inductively coupled plasma emission spectrometer (ICP-OES, SPECTRO BLUE). The lithium recovery was calculated using Equation (1).

$$\eta = \frac{v\rho}{m\gamma} \times 100\% \quad (1)$$

where  $\eta$  represents the lithium recovery,  $v$  represents the volume of the filtrate,  $\rho$  represents the lithium concentration in the filtrate,  $m$  represents the mass of the raw ore,  $\gamma$  represents the lithium content in the raw ore. The tests were conducted in triplicate, and thus, the results presented in this work are average values with the standard deviation.

## 2.3. Characterization

The thermal properties of raw ore were investigated using a thermogravimetric analyzer (STA 8000, perkinelmer, Waltham, MA, USA). Samples were heated from 20 to 800 °C at 10 °C/min with a heating rate in dry oxygen flow of 40 cm<sup>3</sup>/min. The crystalline structure of the sample was studied using X-ray diffraction (X'Pert3 POWder, PANalytical B.V., Almelo, The Netherlands). The Cu K $\alpha$  radiation, nickel filter, and an energy-dispersive one-dimensional array detector were employed, and the scanning rate was set at 8°/min over a range of 2 $\theta$  from 5° to 80°. The XRD instrument operated at 40 kV and 40 mA. The surface morphology of the sample was characterized using a scanning electron microscope, with the SEM HV set at 15.0 kV (TESCAN MIRA3, TESCAN, Brno, The Czech Republic).

## 3. Results and Discussion

### 3.1. Calcination Process

The influences of calcination temperature and calcination time were investigated, and the results are shown in Figure 2. The clay mineral samples were calcined for 60 min at temperatures of 400 °C, 500 °C, 600 °C, 700 °C, and 800 °C, as shown in Figure 2a. The lithium recovery at calcination temperatures of 400 °C and 500 °C showed a low value of 4.28% and 8.96%, respectively. Notably, when the calcination temperature was raised to 600 °C, the lithium recovery exhibited a significant increase to 78.01%, which was then stable when the calcination temperature increased further. This is because the elimination of adsorbed and interlayered water dominated at a low temperature while a substantial change in clay minerals properties, such as structural transformation, occurred at a high temperature of 600 °C [12], making it more favorable for lithium extraction. Therefore, the liberation of lithium from the lithium-bearing clay mineral was predominated at a relatively high temperature, and the calcination temperature of 600 °C is determined.

Figure 2b shows the results of calcination of lithium-bearing clay minerals at a temperature of 600 °C for 30 min, 60 min, 120 min, 180 min, and 240 min. It can be observed that the calcination time has little influence on the lithium recovery. The lithium recovery remained stable in the calcination time range from 30 to 240 min. This may be attributed to rapid lithium release from the layered structure of calcinated clay minerals [13]. The calcination time of 60 min is determined.

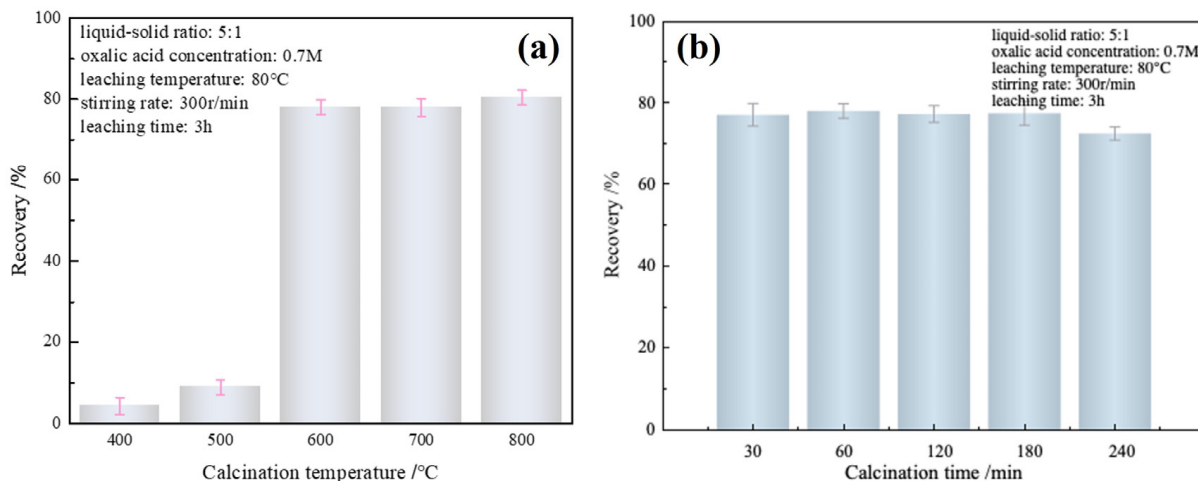


**Figure 2.** Effect of (a) calcination temperature and (b) calcination time on lithium recovery from clay minerals.

### 3.2. Leaching Process

#### 3.2.1. Effect of Stirring Rate

The effect of stirring rate at different leaching times on the lithium recovery from clay minerals is shown in Figure 3, under the conditions of an oxalic acid concentration of 1.2 M, a liquid-to-solid ratio of 8:1, and a leaching temperature of 90 °C. It can be observed that when the stirring rate ranged from 300 rpm to 1200 rpm, the lithium recovery remained stable at approximately 68% at a leaching time of 60 min, and at about 90% at a leaching time of 180 min. Agitation can bring adequate interaction and reaction between the lithium-bearing clay minerals and the oxalic acid solution [14]. Nevertheless, it is indicated that augmenting the stirring speed cannot enhance the leaching rate much, and instead, it led to a greater energy consumption [15]. A stirring speed of 300 rpm can achieve sufficient reaction efficiency. Therefore, the stirring rate is determined to be 300 rpm.

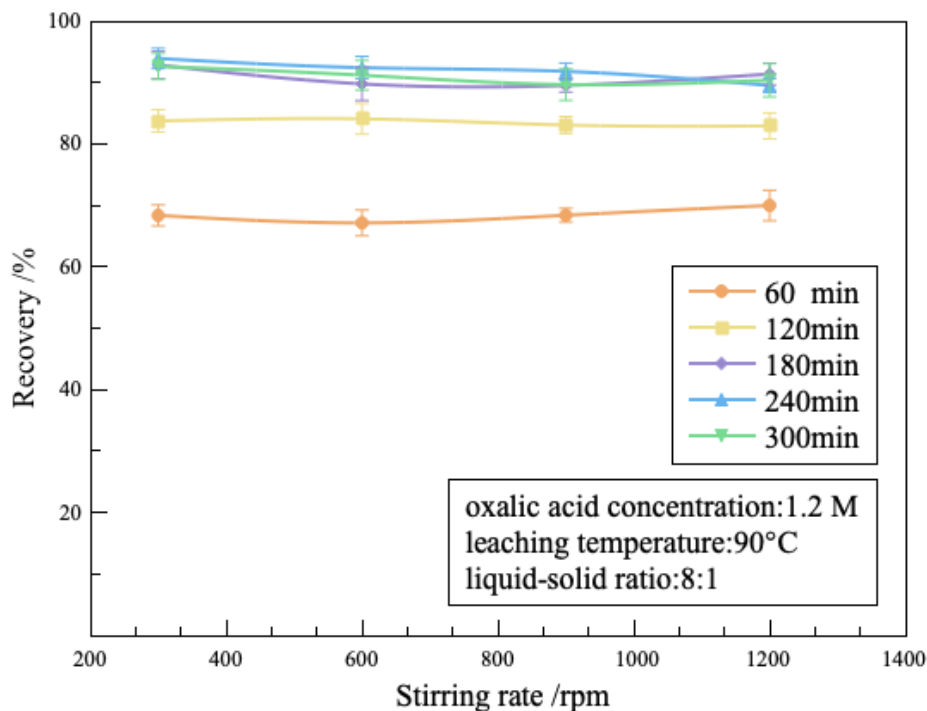


**Figure 3.** Effect of stirring rate on the lithium recovery from clay minerals.

### 3.2.2. Effect of Oxalic Acid Concentrations

The influence of oxalic acid concentration on lithium recovery is shown in Figure 4. It can be observed that, as the oxalic acid concentration increased from 0.4 mol/L to 1.5 mol/L, the lithium recovery gradually increased and remained stable when the leaching time was lower than 2 h. When the leaching time was more than 2 h, the lithium recovery rapidly increased, and then grew slightly as the oxalic acid concentration increased from 0.4 to 1.5 mol/L. Since oxalic acid can dissociate in aqueous solution according to the following equations [16], elevating the oxalic acid concentration facilitates the dissociation of  $H^+$ , which consequently promotes the leaching of lithium. In comparison, similar lithium recovery was obtained at oxalic acid concentrations of 1.2 mol/L and 1.5 mol/L. Therefore, the optimal oxalic acid concentration is determined to be 1.2 mol/L. Additionally, extending leaching time can help to enhance the lithium recovery. It can be seen that the lithium recovery increased from 60.62% at a leaching time of 1 h to 88.26% at a leaching time of 4 h, when the oxalic acid concentration was 1.2 mol/L. This is probably because the longer leaching period offered ample opportunity for intermolecular interactions and chemical reactions, facilitating the release of more lithium ions from the structure of lithium-bearing clays, which in turn boosts the efficiency of lithium extraction [16].

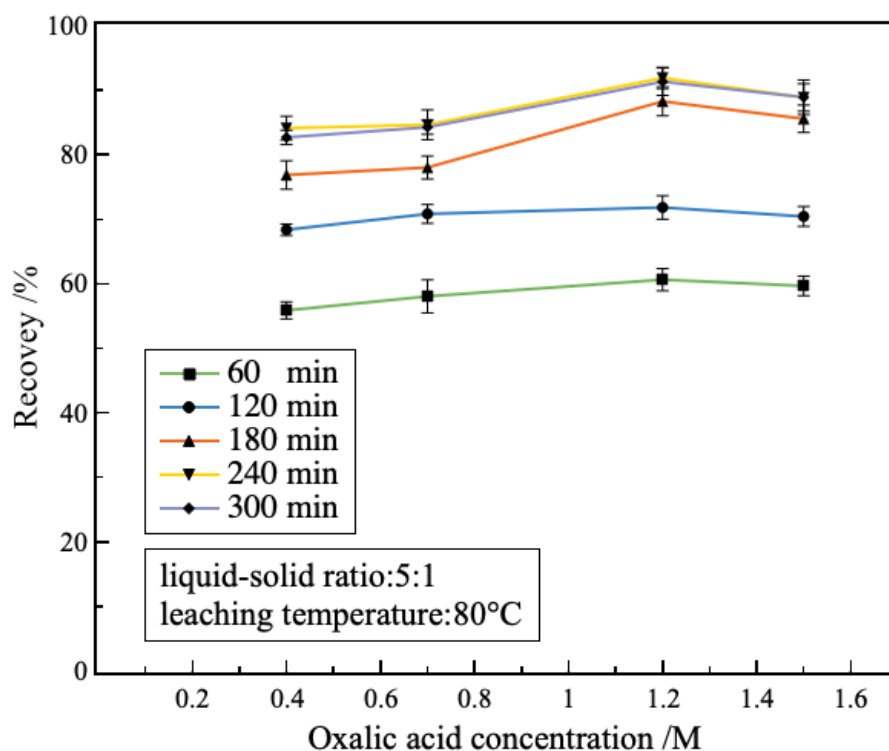
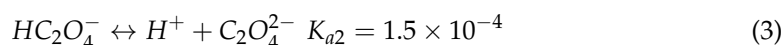
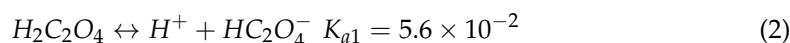


**Figure 4.** Effect of oxalic acid concentration on the lithium recovery from clay minerals.

### 3.2.3. Effect of Liquid–Solid Ratio

Figure 5 illustrates the impact of the liquid–solid ratio on the lithium recovery during leaching process. It is evident that the lithium recovery exhibited a general upward trend with increasing liquid–solid ratio, and kept steady when the liquid–solid ratio was more than 5:1. The lithium recovery reached to 91.35% under the optimal condition of liquid–solid ratio of 8:1 and leaching time of 180 min. Moreover, increasing the liquid–solid ratio can effectively shorten the equilibrium time for lithium recovery. Since elevating the liquid–solid ratio promotes the dissolution of lithium from clay ore, offering ample reaction

space for interaction with oxalic acid and improving the rate of lithium leaching [17]. Nonetheless, excessively high liquid–solid ratios can yield a barely significant improvement in the lithium recovery and result in additional wastage of the oxalic acid. Therefore, the optimal liquid–solid ratio was determined to be 8:1.

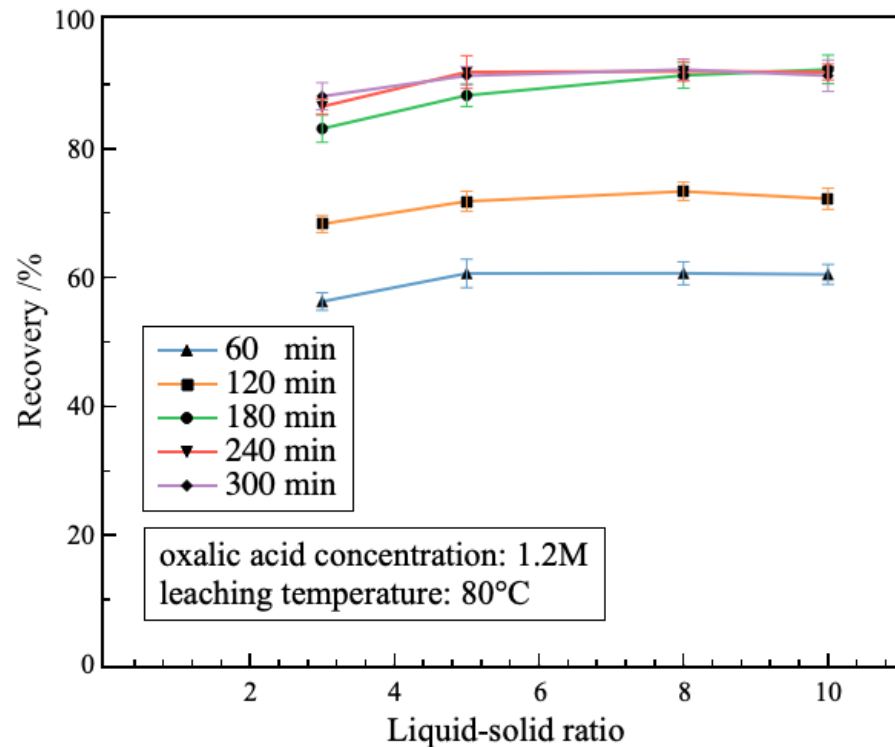


**Figure 5.** Effect of liquid–solid ratio on lithium recovery from clay minerals.

#### 3.2.4. Effect of Leaching Temperature

The effect of leaching temperature at different leaching times on the lithium recovery is shown in Figure 6. The lithium recovery exhibited a direct correlation with increasing leaching temperature. The lithium recovery rose rapidly with the increase in leaching temperature. In particular, the rise in leaching temperature could enhance the leaching efficiency. At leaching temperatures of 50 °C and 60 °C, the lithium recovery after 180 min of leaching time reached between 37.61% and 58.87%, respectively. Further increasing leaching temperature to more than 80 °C, the lithium recovery significantly elevated and then remained stable. This is probably because the temperature during the leaching process typically influenced both the rate of the leaching reaction and the rate of diffusion [18]. As the temperature rose, the energy associated with particle agglomeration also increased, thereby improving the capacity to disrupt or attenuate the crystal lattice within the mineral [19]. This resulted in a greater number of molecules possessing kinetic energy that met or surpassed the threshold of the activation energy, consequently accelerating the leaching process and improving the rate of lithium extraction per unit of time [20]. Furthermore, a rise in temperature led to an increased molecular thermal motion rate, which, in turn, quickened the dissociation of oxalic acid. This process facilitated a greater exchange of H<sup>+</sup> ions with Li<sup>+</sup> ions within the lithium-bearing clay minerals, effectively extracting Li<sup>+</sup> from the silicate layers. Therefore, the temperature of 80 °C was selected as the optimal condition, at which the lithium recovery could reach to 91.35%.

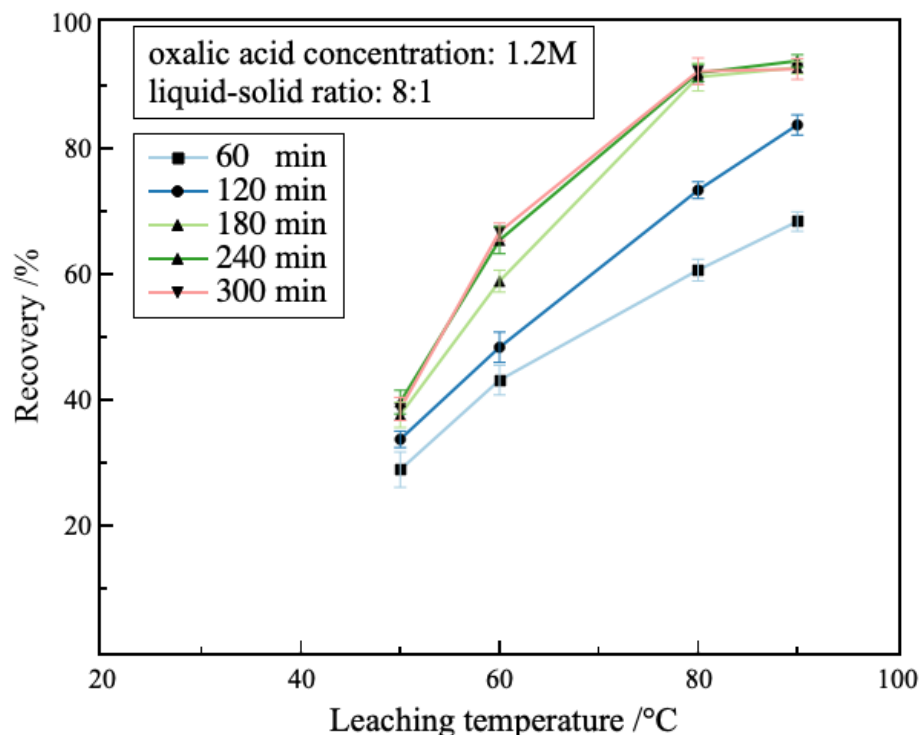


Figure 6. Effect of leaching temperatures on the lithium recovery from clay minerals.

### 3.2.5. Leaching Kinetics

The leaching process of calcined lithium-bearing clay minerals using oxalic acid is a regular heterogeneous liquid-solid non-catalytic reaction. The calcined clay minerals were selectively leached as they reacted with oxalic acid, and a certain amount of solid residue was produced during the leaching process. According to the kinetic principle of hydrometallurgy, when some minerals in the raw materials cannot be leached and solid products are formed, a shrinking core model was used to reveal the reaction type of this leaching process. The following steps are often considered in the leaching process in heterogeneous models: (1) diffusion through the solid product layers (internal diffusion control); (2) control of the reaction by the surface chemistry (chemical reaction control); (3) control of mixed reactions. The rate equations for chemical, diffusion, and mixed reactions are given using Equations (4)–(6), respectively.

$$1 - (1 - \alpha)^{\frac{1}{3}} = k_1 t \tag{4}$$

$$1 - \frac{2}{3}\alpha - (1 - \alpha)^{\frac{2}{3}} = k_2 t \tag{5}$$

$$\frac{1}{3}\ln(1 - \alpha) + (1 - \alpha)^{-\frac{1}{3}} - 1 = k_3 t \tag{6}$$

in which  $\alpha$  represents the lithium leaching rate ( $\eta$  (%)),  $t$  is the leaching time (h), and  $k_1, k_2, k_3$  are all rate control constants.

The chemical reaction equation for the leaching process is shown in Equation (7).



The experimental data on leaching at various oxalic acid concentrations and temperatures were fitted with the kinetic equation mentioned above. The plots of the fitting curve for  $1 - (1 - \alpha)^{\frac{1}{3}}, 1 - \frac{2}{3}\alpha - (1 - \alpha)^{\frac{2}{3}},$  and  $\frac{1}{3}\ln(1 - \alpha) + (1 - \alpha)^{-\frac{1}{3}} - 1$  over time at various oxalic acid concentrations using the governing equation of chemical reactions (4)~(6) are depicted in Figure 7. And Table 1 displays the rate control constants and correlation coeffi-

cients for the various models. As illustrated, the chemical reaction control model exhibited overall a higher regression coefficient  $R^2$  than that of the internal control diffusion and the external control diffusion. The control step in the process of determining the oxalic acid leaching of lithium from calcined clay minerals at oxalic acid concentrations of 1.2~1.5 M was chemical reaction control.

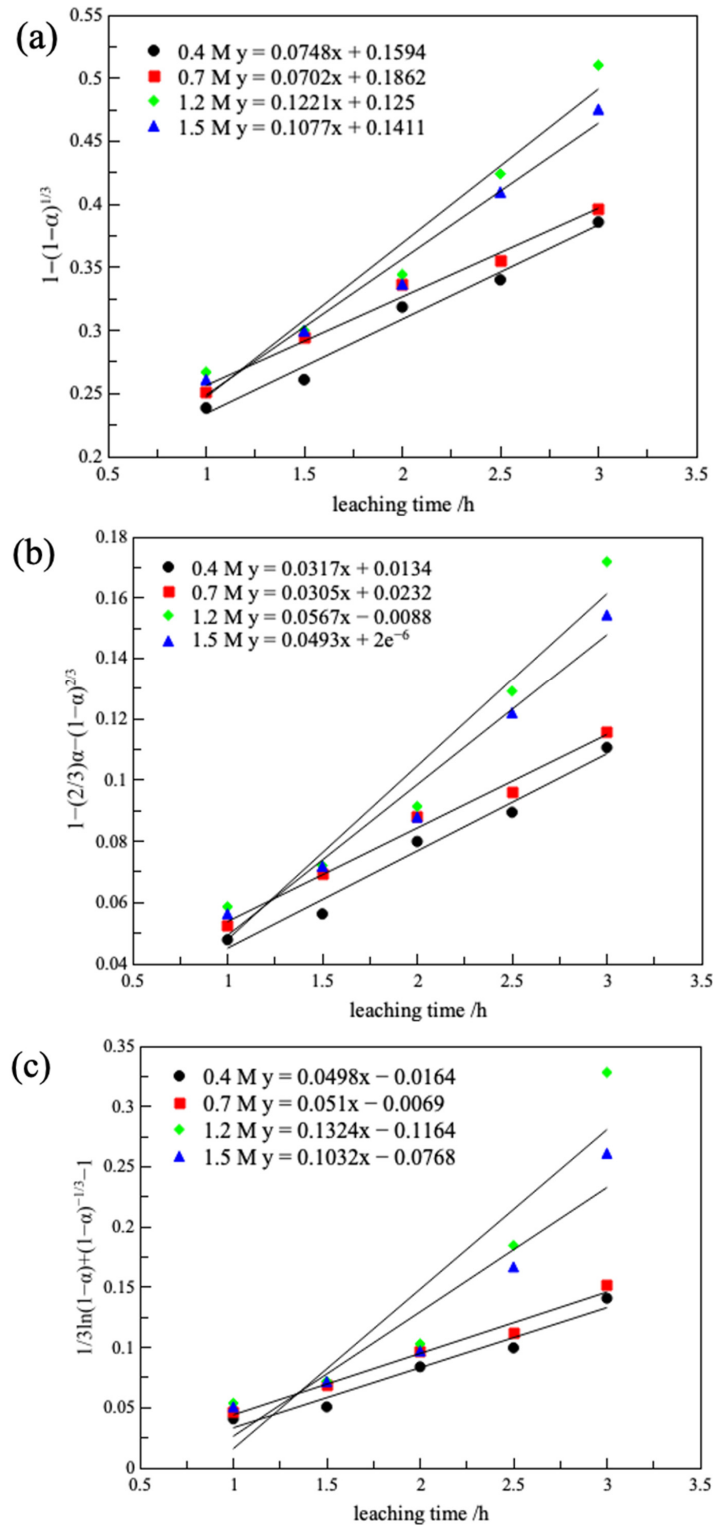


**Figure 7.** Graph of the relationship between the fitted model and time at different oxalic acid concentrations: (a) chemical reaction control, (b) internal diffusion control, and (c) mixed reaction control.

**Table 1.** The rate control constants and correlation coefficients for dynamic models at each oxalic acid concentration.

Oxalic Acid Concentration/(M)	Chemical Reaction Control $1 - (1 - \alpha)^{\frac{1}{3}}$		Internal Diffusion Control $1 - \frac{2}{3}\alpha - (1 - \alpha)^{\frac{2}{3}}$		Mixed Reaction Control $\frac{1}{3}\ln(1 - \alpha) + (1 - \alpha)^{-\frac{1}{3}} - 1$	
	$k_1$	$R^2$	$k_2$	$R^2$	$k_3$	$R^2$
0.4	0.0748	0.987	0.0317	0.979	0.0498	0.962
0.7	0.0702	0.985	0.0305	0.988	0.051	0.981
1.2	0.1221	0.961	0.0567	0.948	0.1324	0.867
1.5	0.1077	0.977	0.0493	0.966	0.1032	0.908

The plots of the fitting curve for  $1 - (1 - \alpha)^{\frac{1}{3}}$ ,  $1 - \frac{2}{3}\alpha - (1 - \alpha)^{\frac{2}{3}}$ , and  $\frac{1}{3}\ln(1 - \alpha) + (1 - \alpha)^{-\frac{1}{3}} - 1$  over time at various temperatures using the governing equation of chemical reactions (4)~(6) are depicted in Figure 8. And Table 2 displays the rate control constants and correlation coefficients for the various models. As illustrated, the chemical reaction control model exhibited a higher regression coefficient  $R^2$  than that of the internal control diffusion and the external control diffusion at the temperature of 333~353 K. The control step in the process of determining the oxalic acid leaching of lithium from calcined clay minerals at 333~353 K was chemical reaction control.

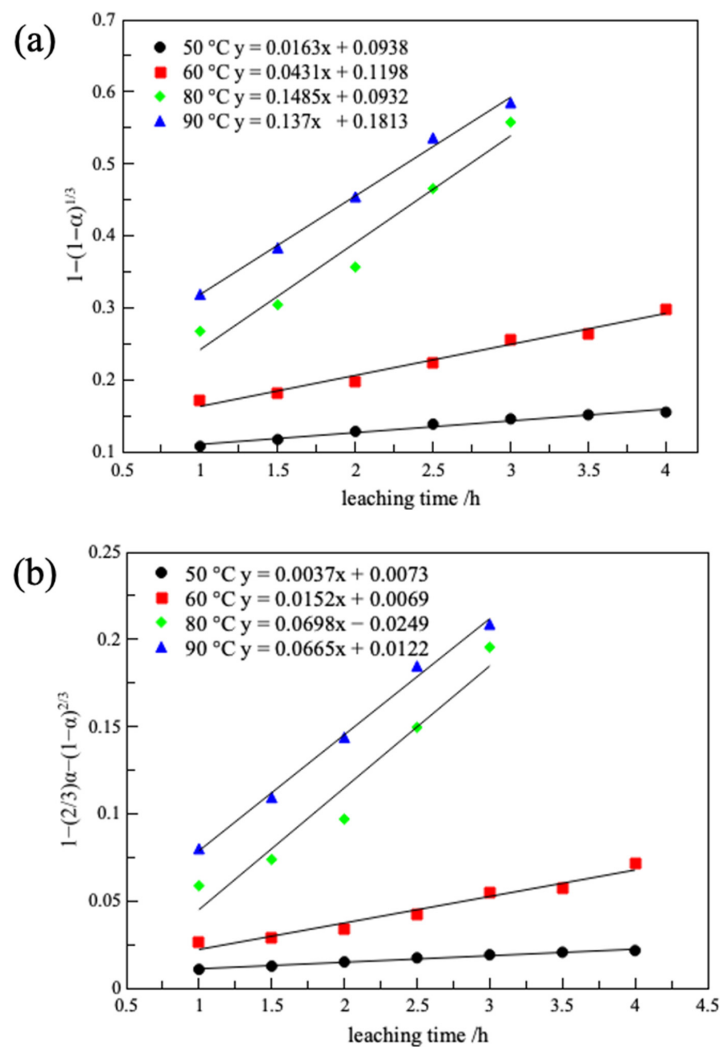


**Figure 8.** Cont.

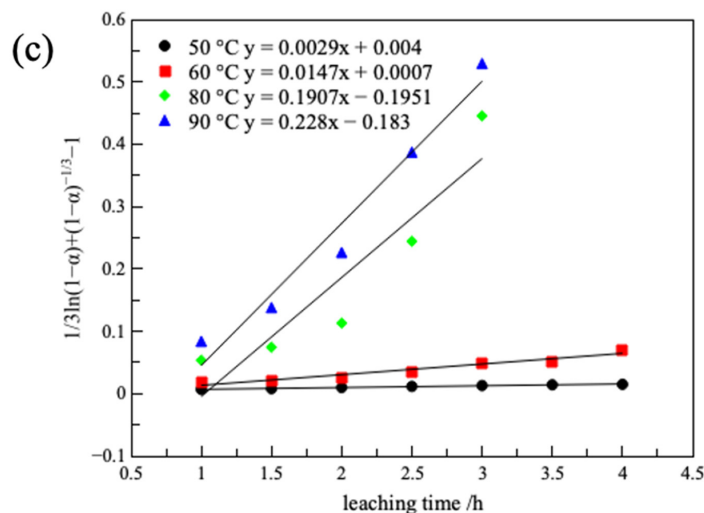


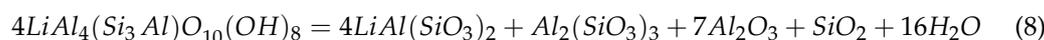
**Figure 8.** Graph of the relationship between the fitted model and time at different temperatures: (a) chemical reaction control, (b) internal diffusion control, and (c) mixed reaction control.

**Table 2.** The rate control constants and correlation coefficients for dynamic models at each temperature.

Temperature/(K)	Chemical Reaction Control $1 - (1 - \alpha)^{\frac{1}{3}}$		Internal Diffusion Control $1 - \frac{2}{3}\alpha - (1 - \alpha)^{\frac{2}{3}}$		Mixed Reaction Control $\frac{1}{3}\ln(1 - \alpha) + (1 - \alpha)^{-\frac{1}{3}} - 1$	
	$k_1$	$R^2$	$k_2$	$R^2$	$k_3$	$R^2$
323	0.0163	0.973	0.0037	0.983	0.0029	0.987
333	0.0431	0.977	0.0152	0.966	0.0147	0.949
353	0.1485	0.960	0.0698	0.948	0.1907	0.857
363	0.137	0.995	0.0665	0.994	0.228	0.963

### 3.3. Lithium Extraction Mechanism

The thermal properties of the lithium-bearing clay minerals and phase transformation during the calcination process at various temperatures of the lithium-bearing clay mineral were investigated using the DTA-TGA (Figure 9a) and XRD analysis (Figure 9b). As shown in Figure 9a, the initial mass loss of about 1% occurred at around 77 °C, which can probably be attributed to the removal of adsorbed water from the clay mineral [21]. The clay mineral underwent a considerable weight reduction in the temperature range of 400 °C to 600 °C, exhibiting the most substantial rate of weight loss at 522 °C [22]. The substantial mass loss of 10% at 522 °C was associated with the release of structural water from the interlayers [21]. And then the interlayer cations migrated to the vacant positions created by -OH groups to satisfy their coordination requirements [23]. A total weight loss reached 12.89% at 796 °C. As shown in Figure 9b, the phases composition of the samples calcined at 400 °C and 500 °C remained relatively unchanged compared with the raw ores, involving chlorite, boehmite, kaolinite, diaspore, and muscovite. As the calcination temperature increased to 600 °C, the peak intensity for kaolinite, boehmite, and diaspore diminished, accompanied by the formation of corundum, quartz, and muscovite. This may result from the solid phase transformation during the calcination process, according to Equation (8).



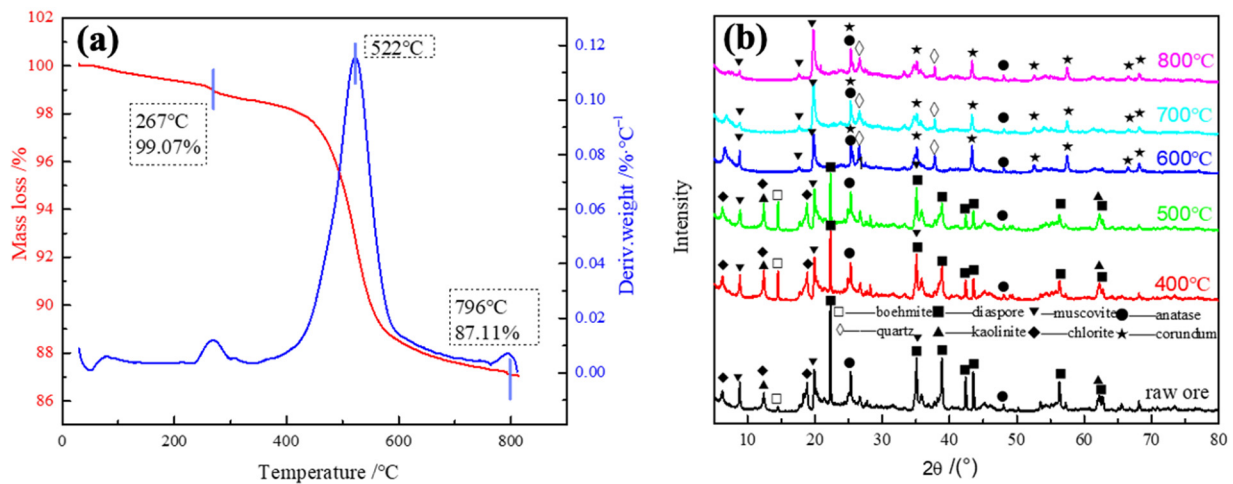


**Figure 9.** (a) DTA-TGA of the raw ore and (b) XRD results of the raw ore and products obtained after calcination process.

During the leaching process, the phase composition of the samples obtained under the condition of various oxalic acid concentration was studied, and the results are shown in Figure 10. As illustrated, the samples obtained at different oxalic acid concentrations shared similar mineral compositions. This is probably because the calcinated ore comprised mainly muscovite, quartz and corundum phases, which cannot react with oxalic acid during the leaching process. Also, it could indicate that, during the leaching process, the dissociated H<sup>+</sup> from oxalic acid engaged in ion exchange with the Li<sup>+</sup> present in the layered silicates [24]. The surface morphology of the raw ore, calcinated ore, and the leaching residue was investigated, and the results are shown in Figure 11. It can be seen that the layered silicate structure of the calcinated clay minerals was destroyed during the leaching process, but the crystal aggregation occurred after leaching process [25]. This is because the Li<sup>+</sup> present on the surface of the separated silicate mineral layers was leached out through ion exchange, and some oxalate ions were adsorbed on the surface of clay minerals [26], promoting the aggregation of mineral grains.

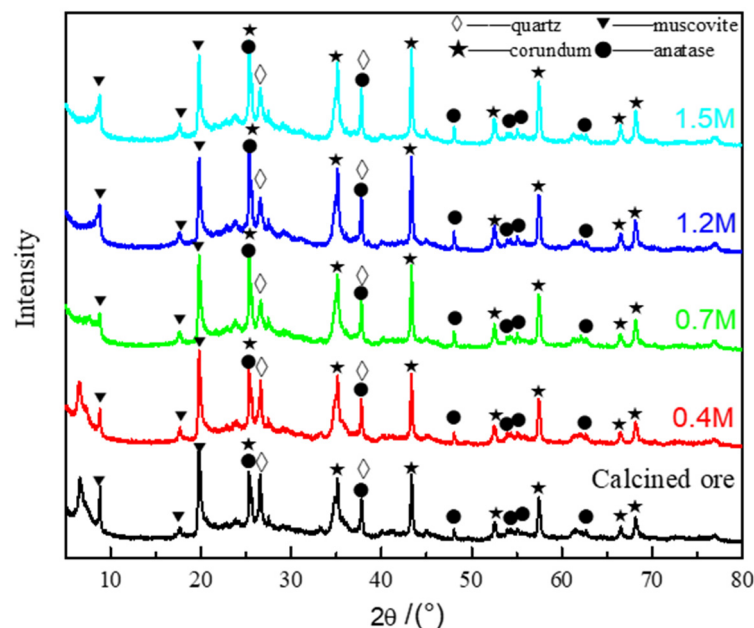


**Figure 10.** XRD results of the calcined ore and leaching residue under various oxalic concentration conditions.

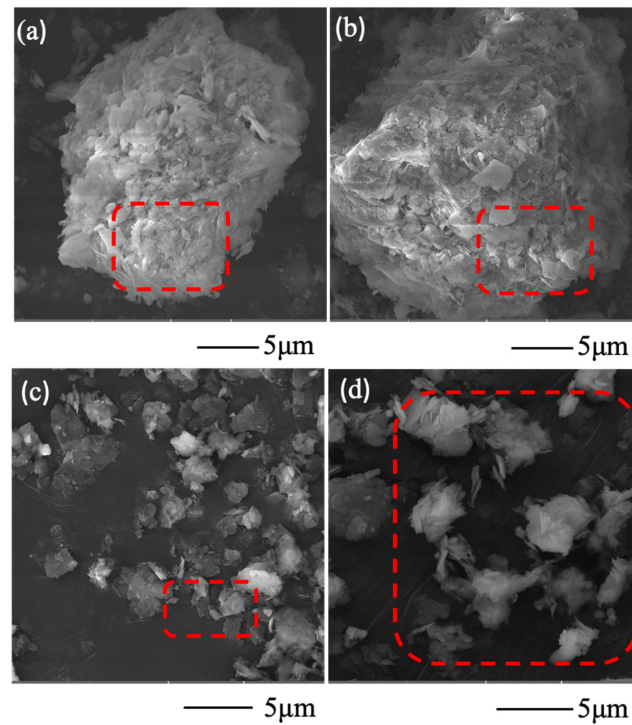


**Figure 11.** SEM images of (a) the raw ore, (b,c) calcined ore at 600 °C, and (d) leaching residue obtained under optimal conditions.

The results of the lithium extraction mechanism from lithium-bearing clay minerals are illustrated in Figure 12. During the calcination process, the layered structure of the clay mineral underwent partial destruction. Due to the expansion of the interlayer spacing of minerals during the calcination process, lithium can be released more easily. During the leaching process, the dissociated  $H^+$  from oxalic acid engaged in ion exchange with the  $Li^+$  present in the layered silicates, resulting in the extraction of lithium from lithium-bearing clay minerals.

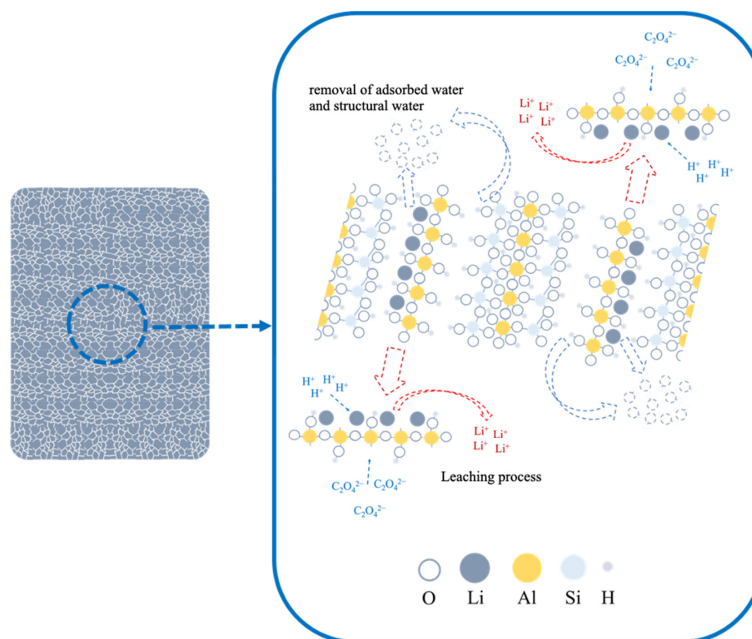


**Figure 12.** Schematic diagram of the calcination-leaching process for lithium extraction from lithium-bearing clay minerals.

#### 4. Conclusions

This study achieved a high recovery of lithium (91.35%) from a lithium-bearing clay mineral in Yunnan Province, China, under the optimal condition of calcination temperature of 600 °C, calcination time of 60 min, leaching temperature of 80 °C, leaching time of 180 min, oxalic acid concentration of 1.2 M, and liquid–solid ratio of 8:1. According to the shrinkage core model, the leaching kinetics of lithium using oxalic acid followed a chemical reaction-controlled process.

TG analysis showed a substantial mass loss of 10% at 522 °C, which was associated with the release of structural water from the interlayers. According to the XRD analysis, the calcination process plays a crucial role in disrupting the layered structure of the clay mineral, leading to the phase transformation from kaolinite, boehmite, and diaspore in raw ore to corundum, quartz, and muscovite in calcination products. During the leaching process, the minerals phase hardly changed, and thus the lithium present in the layered silicates was efficiently recovered through ion exchange with the dissociated H<sup>+</sup> from oxalic acid. This study presents a novel approach involving a sequential process of calcination followed by organic acid leaching, which holds significant implications for the lithium extraction from lithium-bearing clay minerals.

**Author Contributions:** Conceptualization, J.L., R.X., W.S. and L.W.; Methodology, J.L., L.W. and Y.Z.; Formal analysis, J.L. and Y.Z.; Investigation, J.L.; Resources, L.W. and W.S.; Writing—original draft, J.L.; Writing—review & editing, Y.Z.; Supervision, L.W. and Y.Z.; Funding acquisition, L.W. and W.S. All authors have read and agreed to the published version of the manuscript.

**Funding:** This research was funded by the National Natural Science Foundation of China (51974365, 52274285), the National Key R&D Program of China (No. 2022YFC2904401, 2020YFC1908802), the Outstanding Youth Fund of Hunan Natural Science Foundation (2021JJ20064), the Young Elite Scientists Sponsorship Program by CAST (Grant No. 2019QNRC001), and the Innovation-Driven Project of Central South University (No. 2020CX039).

**Data Availability Statement:** Data are contained within the article.

**Acknowledgments:** We are grateful to reviewers for their critical and constructive review.

**Conflicts of Interest:** The authors declare that they have no known competing financial interests or personal relationships that could have appeared to influence the work reported in this paper.

#### References

1. Zhang, Y.; Xu, R.; Sun, W.; Wang, L.; Tang, H. Li extraction from model brine via electrocoagulation: Processing, kinetics, and mechanism. *Sep. Purif. Technol.* **2020**, *250*, 117234. [[CrossRef](#)]
2. Tarascon, J.M. Is lithium the new gold? *Nat. Chem.* **2010**, *2*, 510. [[CrossRef](#)]
3. Peiró, L.T.; Méndez, G.V.; Ayres, R.U. Lithium: Sources, Production, Uses, and Recovery Outlook. *Jom* **2013**, *65*, 986–996. [[CrossRef](#)]
4. Seredin, V.V.; Tomson, I.N. The West Primorye noble-rare metal zone: A new Cenozoic metallogenic taxon in the Russian Far East. *Dokl. Earth Sci.* **2008**, *421*, 745–750. [[CrossRef](#)]
5. Crocker, L.; Lien, R.H. *Lithium and Its Recovery from Low-Grade Nevada Clays*; Bureau of Mines, Department of Interior: Washington, DC, USA, 1987; pp. 8–9.
6. Amer, A.M. The hydrometallurgical extraction of lithium from egyptian montmorillonite-type clay. *Jom* **2008**, *60*, 55–57. [[CrossRef](#)]
7. May, J.T.; Witkowsky, D.S.; Seidel, D.C. *Extracting Lithium from Clays by Roast-Leach Treatment*; Bureau of Mines: Washington, DC, USA, 1980.
8. Gu, H.; Guo, T.; Wen, H.; Luo, C.; Cui, Y.; Du, S.; Wang, N. Leaching efficiency of sulfuric acid on selective lithium leachability from bauxitic claystone. *Miner. Eng.* **2020**, *145*, 106076. [[CrossRef](#)]
9. Zhang, W.; Noble, A.; Yang, X.; Honaker, R. Lithium leaching recovery and mechanisms from density fractions of an Illinois Basin bituminous coal. *Fuel* **2020**, *268*, 117319. [[CrossRef](#)]
10. Li, L.; Dunn, J.B.; Zhang, X.X.; Gaines, L.; Chen, R.J.; Wu, F.; Amine, K. Recovery of metals from spent lithium-ion batteries with organic acids as leaching reagents and environmental assessment. *J. Power Sources* **2013**, *233*, 180–189. [[CrossRef](#)]
11. Li, S.Y.; Zhao, W.; Zhou, Z.F.; Cui, X.L.; Shang, Z.C.; Liu, H.N.; Zhang, D.Q. Studies on Electrochemical Performances of Novel Electrolytes for Wide-Temperature-Range Lithium-Ion Batteries. *ACS Appl. Mater. Interfaces* **2014**, *6*, 4920–4926. [[CrossRef](#)]

12. Irassar, E.F.; Bonavetti, V.L.; Castellano, C.C.; Trezza, M.A.; Rahhal, V.F.; Cordoba, G.; Lemma, R. Calcined illite-chlorite shale as supplementary cementing material: Thermal treatment, grinding, color and pozzolanic activity. *Appl. Clay Sci.* **2019**, *179*, 105143. [[CrossRef](#)]
13. Caritat, P.D.; Hutcheon, I.; Walshe, J. Chlorite Geothermometry: A Review. *Clays Clay Miner.* **1993**, *41*, 219–239. [[CrossRef](#)]
14. Abdeldayem, O.M.; Al Noman, M.A.; Dupont, C.; Ferras, D.; Ndiaye, L.G.; Kennedy, M. Hydrothermal carbonization of Typha australis: Influence of stirring rate. *Environ. Res.* **2023**, *236*, 116777. [[CrossRef](#)]
15. Li, W.; Guo, H.; Huang, Q.; Han, P.; Hou, Y.; Zou, W. Effect of stirring rate on microstructure and properties of microporous mullite ceramics. *J. Mater. Process. Technol.* **2018**, *261*, 159–163. [[CrossRef](#)]
16. Liu, Q.; Tu, T.; Guo, H.; Cheng, H.; Wang, X. High-efficiency simultaneous extraction of rare earth elements and iron from NdFeB waste by oxalic acid leaching. *J. Rare Earths* **2021**, *39*, 323–330. [[CrossRef](#)]
17. Zhang, Y.; Hu, Y.; Sun, N.; Khoso, S.A.; Wang, L.; Sun, W. A novel precipitant for separating lithium from magnesium in high Mg/Li ratio brine. *Hydrometallurgy* **2019**, *187*, 125–133. [[CrossRef](#)]
18. Zhu, K.; He, Y.; Feng, D.; Jiang, W.; Zhang, K. Leaching behavior of copper tailings solidified/stabilized using hydantoin epoxy resin and red clay. *J. Environ. Manag.* **2023**, *345*, 118876. [[CrossRef](#)]
19. Zhou, F.; Zhang, Y.; Liu, Q.; Huang, S.; Wu, X.; Wang, Z.; Zhang, L.; Chi, R. Modified tailings of weathered crust elution-deposited rare earth ores as adsorbents for recovery of rare earth ions from solutions: Kinetics and thermodynamics studies. *Miner. Eng.* **2023**, *191*, 107937. [[CrossRef](#)]
20. Smith, I.W.M. (Ed.) Chapter 3—Molecular collision dynamics. In *Kinetics and Dynamics of Elementary Gas Reactions*; Butterworth-Heinemann: Oxford, UK, 1980; pp. 59–109.
21. Cheng, H.; Yang, J.; Liu, Q.; He, J.; Frost, R.L. Thermogravimetric analysis–mass spectrometry (TG–MS) of selected Chinese kaolinites. *Thermochim. Acta* **2010**, *507–508*, 106–114. [[CrossRef](#)]
22. Zhan, L.; Xia, F.; Ye, Q.; Xiang, X.; Xie, B. Novel recycle technology for recovering rare metals (Ga, In) from waste light-emitting diodes. *J. Hazard. Mater.* **2015**, *299*, 388–394. [[CrossRef](#)]
23. Bailey, S.W. (Ed.) Chapter 10. Chlorites: Structures and crystal chemistry. In *Hydrous Phyllosilicates (Exclusive of Micas)*; De Gruyter: Berlin, Germany, 1988; pp. 347–404.
24. Subramanian, N.; Lammers, L.N. Thermodynamics of ion exchange coupled with swelling reactions in hydrated clay minerals. *J. Colloid. Interface Sci.* **2022**, *608*, 692–701. [[CrossRef](#)]
25. Yang, X.; An, C.; Feng, Q.; Boufadel, M.; Ji, W. Aggregation of microplastics and clay particles in the nearshore environment: Characteristics, influencing factors, and implications. *Water Res.* **2022**, *224*, 119077. [[CrossRef](#)] [[PubMed](#)]
26. Martial, N.G.; Yao, S.; Hamer, U.; Zhang, Y.; Zhang, B. Positive and negative priming effects induced by freshly added mineral-associated oxalic acid in a Mollisol. *Rhizosphere* **2023**, *26*, 100708. [[CrossRef](#)]

**Disclaimer/Publisher’s Note:** The statements, opinions and data contained in all publications are solely those of the individual author(s) and contributor(s) and not of MDPI and/or the editor(s). MDPI and/or the editor(s) disclaim responsibility for any injury to people or property resulting from any ideas, methods, instructions or products referred to in the content.